

1 **Effect of concrete carbonation on phosphate removal through adsorption**  
2 **process and its potential application as fertilizer**

3  
4 Glaydson S. dos Reis<sup>1,2</sup>, Pascal S. Thue<sup>1</sup>, Bogdan G. Cazacliu<sup>2</sup>, Eder Claudio Lima<sup>1</sup>,  
5 Carlos Hoffmann Sampaio<sup>3</sup>, Marco Quattrone<sup>1</sup>, Ekaterina Ovsyannikova<sup>4</sup>, Andrea  
6 Kruse<sup>4</sup>, Guilherme Luiz Dotto<sup>1</sup>

7  
8  
9 <sup>1</sup> Graduate Program in Metallurgical, Mine, and Materials Engineering (PPGE3M). School of  
10 Engineering, Federal University of Rio Grande do Sul (UFRGS), Center of Technology, Porto  
11 Alegre, RS, Brazil.

12 <sup>2</sup> IFSTTAR, MAST, GPEM, F-44344 Bouguenais, France.

13 <sup>3</sup> Professor Serra Húnter Program, Department of Mine, Industrial and ICT Engineering,  
14 Polytechnical University of Catalonia, Av. Bases de Manresa 61–63, Manresa, 08242 Barcelona,  
15 Spain.

16 <sup>4</sup> Department of Conversion Technologies of Biobased Resources, Institute of Agricultural  
17 Engineering, University of Hohenheim, Garbenstrasse 9, 70599 Stuttgart, Germany

18  
19  
20  
21 *\*Corresponding author: FAX + 55 (51) 3308 7070; Phone: +55 (51) 3308 7070; e-mail:*  
22 *[glaydsonambiental@gmail.com](mailto:glaydsonambiental@gmail.com)*

## Abstract

Concrete slurry is an abundant, cheap, and commonly found waste all over the world where construction activities take place; concrete slurry which is rich in calcium and metallic oxides could be successfully employed in the phosphate (P) removal from aqueous media. In this research, the effect of the carbonation process over physicochemical properties and in the adsorption of phosphate on the concrete slurry powder was investigated.

The results showed that non-carbonated sample was more effective in the P removal due to higher releasing of  $\text{Ca}^{2+}$  in comparison to carbonated sample. The dissolved  $\text{Ca}^{2+}$  from the dissolution of  $\text{Ca}(\text{OH})_2$ ,  $\text{CaCO}_3$ , and  $\text{CaO}$  are preferably precipitated by phosphates in high pH solution, reflecting in a high initial adsorption rates.

General order kinetic and Liu isotherm provided the better fitting models for the adsorption behavior of P onto both non-carbonated and carbonated concrete samples. Phosphate removal was mainly ruled by chemical adsorption through inner-sphere complexation and P precipitation on the surface of the adsorbent containing  $\text{Ca}^{2+}$  as an essential element in the adsorption mechanism. Compared with other phosphate adsorbents, both non-carbonated and carbonated concrete may be an economical and efficient adsorbent.

The non-carbonated sample gave a high adsorption capacity of P ( $47.6 \text{ mg g}^{-1}$ ) and presenting fast and high initial adsorption, reaching 72% of P removal within 5 minutes (min) at  $22^\circ\text{C}$ , while carbonated showed adsorption capacity of  $30.6 \text{ mg g}^{-1}$ , at the same experimental conditions. Therefore, concrete slurries can be used widely as an inexpensive phosphate-recovery adsorbent.

Besides, the application of these loaded P waste, as potential fertilizers in soil can be an exciting and environmentally approach for reusing this solid-waste. The environmental analysis highlighted that the adsorbents did not leach out chemicals above the allowable limits preconized by FAO for irrigation waters. However, aspects

53 related to monitoring the presence and mobility of heavy metals on soil must be better  
54 addressed and monitored.

55

56 **Keywords:** Recycling slurry concrete; concrete-waste adsorbent; phosphate adsorption;  
57 potential fertilizer.

58

## 59 **1. Introduction**

60

61 Concrete is the most used popular material throughout the construction industry  
62 due to the several matters such as availability, accessibility, durability, and economic  
63 issues associated with its production and use (WBCSD 2019). However, with the rapid  
64 development of the industry of concrete fabrication all over the world, large quantities of  
65 by-products are produced (WBCSD 2019). The annual global concrete consumption  
66 reaches 25 billion tonnes. This production generates a large number of leftovers of fine  
67 powder slurry of concrete (Aynur and Ulubeyli, 2016). The leftovers are generated from  
68 Internal washing of the balloon of the concrete mixer truck and the washing process of  
69 the yard where the concrete blocks are placed.

70 Although it is difficult to determine precisely the waste volume generated, it is  
71 estimated that every day a concrete batching plant can generate about 0.4-0.5% of new  
72 concrete waste in the relation of its total production (Aynur and Ulubeyli, 2016).  
73 Therefore, it is imperative to explore the potential recycling of this type of fresh concrete,  
74 which the recovery and reuse of both fine aggregates and water can bring several  
75 benefits to the economic and environmental point of views (Aynur and Ulubeyli, 2016).

76 Over past few years, many types of reuse for slurry concrete have been  
77 proposed, such as concrete production itself (Bravo et al., 2018), mortar and ceramic  
78 materials (Cardoso et al., 2016), geopolymers synthesis (Vásquez et al., 2016), and  
79 others. However, there is also a high potential for using concrete slurries for  
80 environmental applications as eco-friendly materials. For instance, the concrete slurries

81 can be used as adsorbents for uptake pollutants in aqueous media by adsorption (Wang  
82 et al., 2014).

83 Adsorption is a widespread operation unit in which a specie named as adsorbate  
84 bound at the surface of the adsorbent. This process is a low-cost and effective technique  
85 for the removal of pollutants in aqueous media (dos Reis et al., 2016). An essential  
86 advantage of the adsorption process is that the adsorbents can be regenerated and  
87 reused many times, which makes the process even cheaper compared to others.

88 Sasaki *et al.*, (2014) studied the removal of arsenate in aqueous solution, using  
89 concrete waste as adsorbents. The results showed high adsorption capacity and the  
90 primary adsorption mechanism was ion exchange between arsenic molecules and ions  
91 at the surface and matrix of concrete-waste adsorbents, in which ettringite  
92 ( $\text{Ca}_6\text{Al}_2(\text{SO}_4)_3(\text{OH})_{12}\cdot 26\text{H}_2\text{O}$ ) was at a higher amount. Littler *et al.*, (2013) studied the  
93 adsorption properties of cement/concrete matrix in the removal of phosphate in aqueous  
94 solution. The results obtained appointed that during the adsorption process,  
95 cement/concrete matrix released  $\text{Ca}^{2+}$  in solution, which attracts and bind phosphate  
96 species, resulting in the precipitation reaction in the form of calcium phosphate solids.  
97 The same phenomenon was observed and related by Park *et al.*, (2008).

98 Therefore, herein, it is proposed to evaluate the carbonation of slurry concrete  
99 and its influence on the slurry microstructure properties and how the carbonation process  
100 affects the adsorption of phosphate compounds in aqueous media.

101 Carbonation is a physical-chemical neutralization process as a result of the  
102 absorption of atmospheric  $\text{CO}_2$  in the concrete pores, which reacts with calcium  
103 hydroxide ( $\text{Ca}(\text{OH})_2$ ) and other hydrated compounds of cement matrix to form calcite  
104 ( $\text{CaCO}_3$ ) (Abass and Olajire 2013). Carbonation process can promote important  
105 changings on concrete surface microstructures, which can reflect in the adsorption  
106 properties.

107 The phosphates will be employed as adsorbate in this research. Indeed,  
108 phosphates are a vital nutrient that is essential for life. It is a crucial component added in

109 fertilizers for food production and has no substitute. Therefore, recovering phosphates  
110 from wastewaters are imperative (Sun et al., 2018). Phosphates in surface waters even  
111 at small concentrations can lead to the eutrophication, which poses a considerable risk  
112 to the ecosystem, resulting in environmental as well as economic damage (Sun et al.,  
113 2018). The presence of phosphates in natural waters comes from diffuse sources such  
114 as agricultural run-offs and municipal wastewater treatment plants (Ma et al., 2018).  
115 Hence there is a need for a method that can effectively diminish the phosphates to lower  
116 concentration or eliminate their presence in wastewaters before they are released in the  
117 environment.

118 Therefore, the overarching purpose of this study is to investigate the effect of  
119 progressive carbonation on microstructural and surface properties of the concrete slurry  
120 waste. Then, the presence of functional groups at the microstructure and pore structures  
121 of slurry before and after carbonation is also investigated. Lastly, the potential in the  
122 removal or recovery phosphates from aqueous solutions is tested.

123

## 124 **2. Materials and methods**

125

### 126 ***2.1. Raw material***

127

128 The slurry concrete is generated from the washing of concrete mixer trucks and  
129 it is separated from wastewater as suspended solids at the ready-mixed concrete plants.  
130 The wet sample was collected from wastewater obtained during the washing of the  
131 concrete mixer truck ballons immediately after being discharged into the sedimentation  
132 tanks. Two buckets of fresh slurry concrete generated were collected (each one was  
133 about 30 kg of fresh slurry concrete).

134 A few hours later, the slurry of concrete became hardened, due to the hydration  
135 of residual cement. The dry material was then comminuted by a concrete mixer. After

136 homogenization and quartering processes, eight samples of about 100.0 g (passing the  
137 1-mm sieve aperture) were obtained and named according to their ages as follows: 0, 7,  
138 14, 21, 28, 35, 42, 49 and 56 days.

139 All the reagents were analytical grade and used as received without any further  
140 purification. Potassium phosphate dibasic ( $K_2HPO_4$ ) was purchased from Sigma-Aldrich  
141 (DE). Deionized water was used for the preparation of the solutions, and ethanol was  
142 procured from Beijing Chemical Reagents Company (China).

143

## 144 **2.2. Accelerated carbonation process**

145

146 The dried slurry powder concrete (particle size < 1.00 mm) was placed onto  
147 plastic disks and introduced in a carbonation chamber under the following conditions:  
148 temperature of 23°C, CO<sub>2</sub> content of 5% and relative humidity of 65%. A total of eight  
149 samples were conditioned for 8 weeks (56 days), and the effect of carbonation was  
150 evaluated according to their ages, as shown in **Fig. 1**.

151



152

153 **Fig.1** Samples of slurry concrete numbered according to their ages.

154

## 155 **2.3. Slurry concrete characterization**

156 The textural characterisation was carried out using N<sub>2</sub> adsorption-desorption  
157 isotherms at liquid N<sub>2</sub>, using a Tristar II Kr 3020 Micromeritics equipment. Prior analyses,  
158 the samples were degassed at 120 °C under vacuum. The specific surface area was  
159 determined by BET (Brunauer, Emmett and Teller) method (Umpierres et al., 2018).

160 The morphologies and majority elements of the concrete samples were observed  
161 with a scanning electron microscope (SEM) equipped with energy-dispersive X-ray  
162 spectroscopy (EDS) (TESCAN 3, Sweden) (Wamba et al., 2017).

163 The functional groups of the concrete slurry were determined using a Fourier  
164 Transform Infrared Spectroscopy (FTIR) with the ATR (Attenuated Total Reflectance)  
165 accessory, Bruker Spectrometer, alpha model (Thue et al., 2017).

166 Differential thermogravimetric (DTG) analysis was made by using a TA  
167 Instruments model SDT Q600 (New Castle, USA) with a heating rate of 10°C·min<sup>-1</sup> at  
168 100 mL·min<sup>-1</sup> of the synthetic flow of air. The temperature was varied from 20° up to  
169 1000°C (Wamba et al., 2017).

170

#### 171 **2.4. Adsorption tests**

172

173 Several aliquots of 20.00 mL of phosphate solutions with different initial  
174 concentrations ranging from 20.00 to 950.0 mg L<sup>-1</sup> and at initial pH ranging from 2.0 to  
175 12.0 were added into 50.0 mL Falcon tubes containing 0.03 – 0.5g (gram) of concrete-  
176 waste adsorbents. The flasks were capped and placed horizontally in a shaker, and the  
177 system was agitated between 5 min to 4 hours (h) (Leite et al., 2017). Afterward, the  
178 adsorbents were separated from the aqueous solutions by centrifugation using a Fanem  
179 centrifuge. Then the aliquots of 1–5 ml of the supernatant were properly diluted into 10.0–  
180 100.0 ml with a suitable blank solution (Leite et al., 2017).

181 The initial, as well as the residual phosphates concentrations, were quantified  
182 after adsorption experiments by using ICP-OES technique with Agilent 715 equipment.  
183 The content of phosphates adsorbed by the concrete-waste adsorbents and the

184 percentage of phosphates removed was calculated using Eq. 1, also, Eq. 2, respectively  
 185 (Kasperiski et al., 2018):

$$q = \frac{(C_o - C_f)}{m} \cdot V \quad (1)$$

$$\%Removal = 100 \cdot \frac{(C_o - C_f)}{C_o} \quad (2)$$

186 q is the quantity of P ions removed by the concrete adsorbents in mg g<sup>-1</sup> , Co is the initial  
 187 P initial concentration in the solution in mg L<sup>-1</sup> , Cf is the P concentration after the batch  
 188 adsorption experiment in mg L<sup>-1</sup> , m is the mass of concrete adsorbents in g and V is  
 189 the volume of P solutions in contact with the concrete adsorbents in L.

190

#### 191 *2.4.1 Analytical control of the measurements and statistical evaluation*

192 See Supplementary Material and references (Leite et al., 2017; Kasperiski et al.,  
 193 2018).

194

#### 195 *2.4.2. Kinetic of adsorption*

196

197 See Supplementary Material (Lima et al., 2015).

198

#### 199 *2.4.3 Equilibrium of adsorption*

200

201 See Supplementary Material (Lima et al., 2015).

202

### 203 **3. Results and discussion**

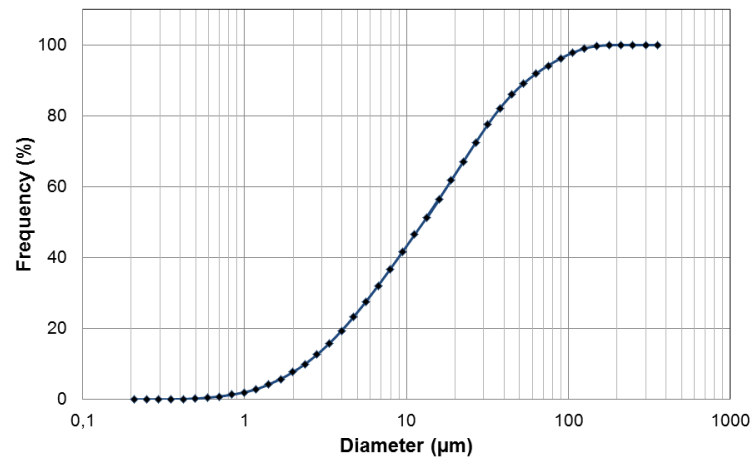
204

#### 205 ***3.1. The particle size distribution of the natural concrete used in the*** 206 ***carbonation experiments***

207



208 **Fig. 2** shows the particle-size distribution (PSD) of the fine fraction ( $\phi < 1.00$  mm)  
 209 used for carbonation experiments. It is possible to see that the particle-size distribution  
 210 analysis of the slurry concrete showed fine and continuous material containing 90% of  
 211 particles lower than  $56 \mu\text{m}$  ( $D_{90}$ ) (See **Fig. 2**). Also, the slurry powder concrete presented  
 212  $D_{50}$  value (which is the particle size in which 50% of the total mass has passed through  
 213 the sieve of  $\phi < 1.00$  mm) of  $12.77 \mu\text{m}$ , and 10% of the material has a size of  $2.37 \mu\text{m}$ .  
 214 Smaller particles might have an influence on the carbonation process and even on the  
 215 kinetic of adsorption and sorption capacity. This is because smaller particles have more  
 216 surface area available to get in contact with the  $\text{CO}_2$  (in the carbonation process) and  
 217 also with the phosphate species during the adsorption experiments. Therefore, lower  
 218 particles sizes can improve the adsorptive properties.  
 219



220

221 **Fig. 2** - Grading curve of the concrete used for carbonation experiments.

222

### 223 **3.2. Specific surface area and porosity**

224

225 The values of the specific surface areas of slurries concrete samples before and  
 226 after carbonation are presented in **Table 1**, that were obtained by nitrogen adsorption-

227 desorption isotherms. In general, the specific areas increased as the carbonation time  
228 also increased. These results justify that the crystallization of calcite minerals creates  
229 new porous surfaces during the carbonation process. In fact, during the carbonation  
230 process, the microstructure of concrete solid expands as the  $\text{Ca}^{2+}$  ions in the interlayer  
231 space progressively decreases due to the reaction between calcium ion and  $\text{CO}_2$ . This  
232 phenomenon will be further explained in section 3.3.

233

234 **Insert table 1**

235

236 Fig. 3 and Table 1 present the distributions of the pore sizes of the slurry samples,  
237 at different days of carbonation. The results show significant differences in the pore size  
238 diameter in two regions; around 10 nm and 90.0 nm. For the non-carbonated slurry (at  
239 zero-day) the incremental porosity was higher in the region around 90 – 100 nm.  
240 However, for the carbonated samples, the incremental porosity was higher in the region  
241 of 10 nm. Looking at Fig. 3A, it seems that as long as the carbonation is progressing the  
242 size of pores became smaller. This statement is strengthening by Fig. 3B, which shows  
243 that the cumulative porosity gradually reduced as carbonation progressed (Taylor 1978).  
244 These changes can have a decisive influence on the adsorption properties of both non-  
245 carbonated and carbonated samples.

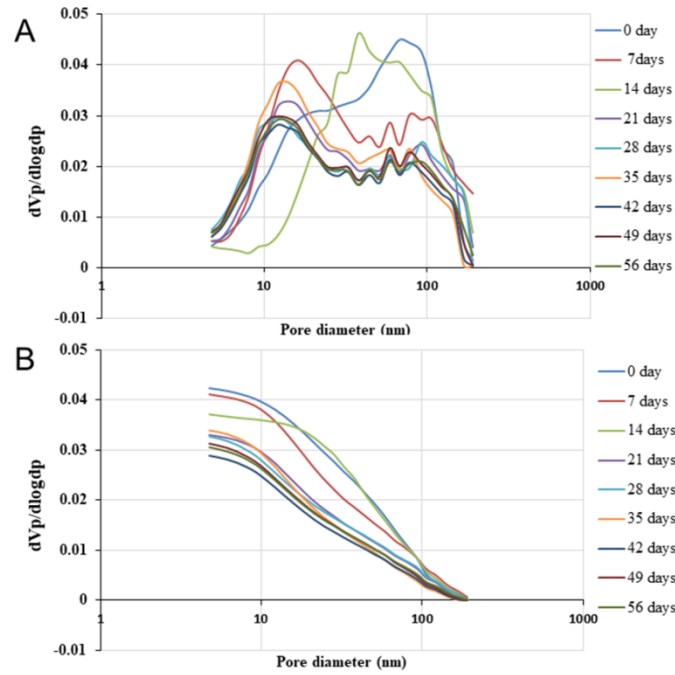
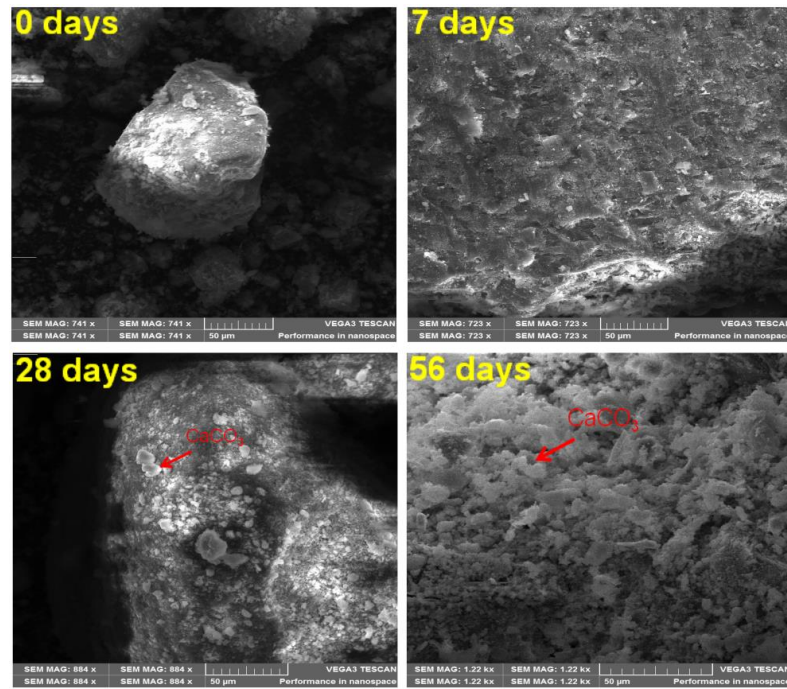


**Fig. 3.** The pore size distribution of carbonated concrete slurry

### 3.3. Surface features of the adsorbent samples

The surface morphology of the carbonated samples revealed by SEM might reinforce what was discussed in section 3.2. The SEM images are shown in the Fig.4. It shows that the surface of the carbonated slurry sample at the 7 days presented a smooth surface where no porosity can be observed. However, as long the carbonation is progressing the surfaces of the carbonated samples get more irregular and rougher (see Fig. 4), which may increase the porosity. This should be attributed to the formation and precipitation of the  $\text{CaCO}_3$  (see red arrow in Fig.5) on the particle surface of slurry concrete due to the carbonation of the hydration products. As can be seen at 56 days of carbonation under given conditions, the surface of slurry concrete is almost totally covered by  $\text{CaCO}_3$ .



261

262

**Fig. 4.** Typical SEM images of the slurry samples at different ages of 0, 7, 28,  
and 56 days of the carbonation process.

263

264

265

266

267

268

269

270

271

272

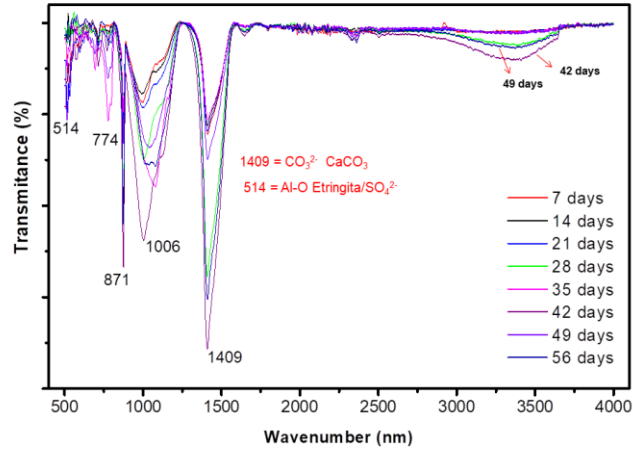
273

274

275

276

Fourier transformation infrared spectroscopy (FTIR) can detect the presence of C–O in the concrete slurry to determine the presence of carbonate ( $\text{CaCO}_3$ ). The spectrum of each slurry sample was determined by ATR, which allow determining the effect of the carbonation through the different ages. The FTIR spectra of non-carbonated and carbonated slurry concrete are shown in Fig. 5. As can be seen, all samples presented similar spectrums, and the main difference is in the intensity of the bands. It is possible to see in Fig. 5 that the bands get more intensive as the carbonation time increased, which might indicate that more carbonate is being formed. The major bands are listed as sulfate band in  $1006\text{ cm}^{-1}$  (Wamba et al., 2017), anhydrous calcium silicates bands in  $514\text{ cm}^{-1}$  while carbonate phases were in  $1409$ ,  $871$  and  $774\text{ cm}^{-1}$  (Wamba et al., 2017).



277

278

**Fig. 5.** FTIR spectrums of the carbonated slurry concrete samples.

279

280

281

282

283

284

285

286

287

288

289

290

291

### **3.4. Derivative thermogravimetric of the concrete samples**

292

293

294

295

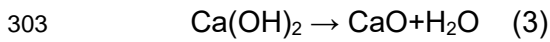
296

297

Derivative thermogravimetric (DTG) analysis has been used as a tool to study the carbonation reaction in concrete material. As we can see in Fig. 6, the first broad peaks between 74° and 106°C for both carbonated samples (28 and 56 days), and non-carbonated sample (0 days) referred to the moisture releases from samples. The second mass loss peak around 455°C correspond to calcium hydroxide dehydration, and it is

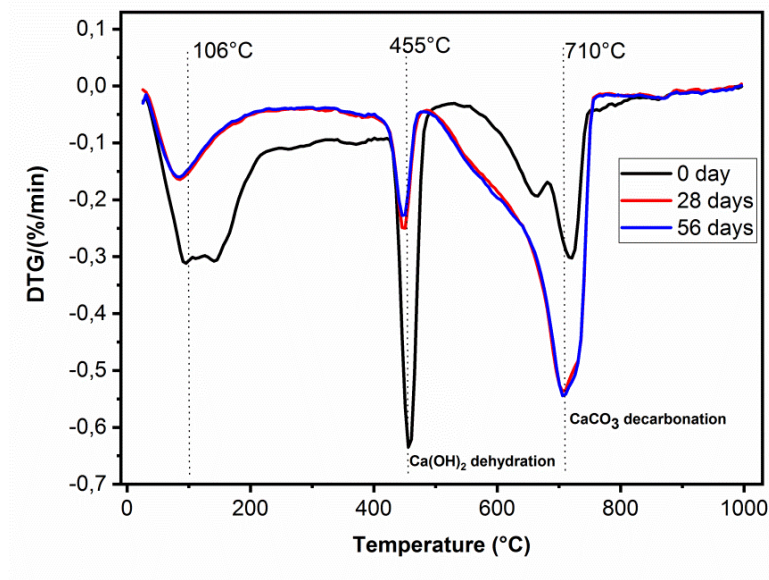
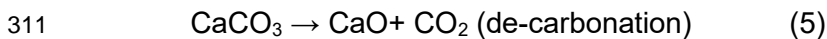
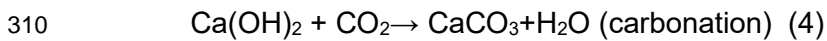
298 typical for the three samples (Tracz and Zdeb, 2019). However, for the non-carbonated  
 299 sample, the peak was more intense, due to the higher content of  $\text{Ca(OH)}_2$ . The  $\text{Ca(OH)}_2$   
 300 dehydration chemical reaction takes place, as shown in the following equation (Tracz  
 301 and Zdeb, 2019):

302



304

305 Finally, the peak at  $710^\circ\text{C}$  corresponds to the decomposition of the carbonates,  
 306 where we can notice more intensive peaks in carbonated samples. A higher amount of  
 307  $\text{CaCO}_3$  is expected in carbonated samples compared to the natural slurry concrete.  
 308 Equation (4) shows the portlandite carbonation reaction, while equation (5) shows the  
 309 de-carbonation equation (Tracz and Zdeb, 2019).



312

313 **Fig. 6** - DTG curves for 0, 28 and 56 days of carbonation

314

### 315 **3.5 Adsorption studies**

316

#### 317 **3.5.1 Effect of Adsorbent Mass**

318

319 The adsorbent dosage in the adsorption step is a crucial factor in making the  
320 adsorption process applicable in real industrial scale.

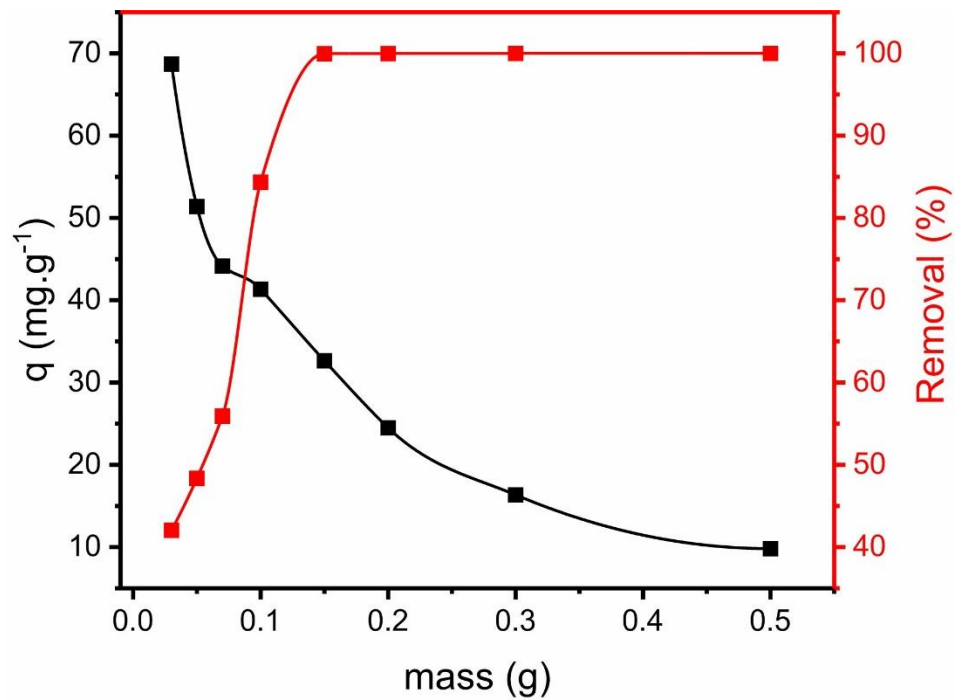
321 **Fig. 7** describes the effect of mass concrete adsorbent (ranging from 0.0300 to  
322 0.5000 g) on P removal using non-carbonated concrete. For the adsorption tests, a fixed  
323 volume of 20.0 mL of P solution at an initial concentration of 240.0 mg L<sup>-1</sup> was used. **Fig.**  
324 **7** shows that the P sorption percentage increases, from 40 to 100%, as the adsorbent  
325 dosage increases, from 0.0300 to 0.1500 g, respectively. Adsorbent masses beyond  
326 0.1500 g keep the percentage removal constant while the amounts of adsorbed P per  
327 unit weight ( $q_e$ ) of the concrete-waste adsorbent decreased when increasing the mass  
328 of solid/volume of solution ratio (see **Fig. 7**).

329 The rapid increase of the P adsorption as the adsorbent dosage increases  
330 indicates the accessibility of a more significant number of sorption sites at a higher  
331 dosage to adsorb P ions (see **Fig. 7**). This result suggests that high numbers of free  
332 adsorption sites were available during the first stage of the process and then, as time  
333 passes, the free remaining sites were less and became more difficult to be occupied due  
334 to repulsive forces between the adsorbate and adsorbent particles (Choi et al., 2016).

335 The most effective adsorption result for phosphate was attained at 0.1000 g with  
336 84.3% of P removal meaning a " $q_e$ " of 41.3 mg·g<sup>-1</sup> while 0.1500 g reached almost 99.2%  
337 but with a " $q_e$ " of 32.6 mg·g<sup>-1</sup> (see **Fig. 7**). The choice of the mass of 0.1000 g to be  
338 considered the most efficacious lies in the fact that 0.1500 g is 50% higher, compared to  
339 0.1000 g, and achieves adsorption capacity only 15% higher. Also, the " $q_e$ " for the 0.1g  
340 is 21.1% higher than 0.15g.

341 Therefore, for further experimental studies, the adsorbent dosage is optimized at  
342 0.1000 g in 20.0 mL of solution (5.00 g L<sup>-1</sup>). Based on the above observations, it becomes  
343 evident that phosphate adsorption is majority a phenomenon of the surface. Indeed the  
344 amount of surface vacant sites for adsorption and therefore the mass of adsorbent can  
345 extensively influence adsorption efficiency.

346



347

348

**Fig. 7.** Effect of adsorbent dosage on P removal using non-carbonated sample

349

(0 days).

350

351

### 3.2.2 Effect of the pH on P removal

352

353

354

Changes in pH may affect the adsorption process either dissociating the adsorbate in different species and functional groups present at the adsorbent's active sites. Thus, it is necessary to know the influence that this parameter has on the process of adsorption of phosphate in aqueous solution.

355

356

357

358

Depending on the pH on the P solution, many phosphates species ( $\text{H}_3\text{PO}_4$ ,  $\text{H}_2\text{PO}_4^-$ ,  $\text{HPO}_4^{2-}$  and  $\text{PO}_4^{3-}$ ) can be present at different proportions (Xie et al., 2014). **Fig. 8** shows the influence of pH on P removal by both samples (0 and 56 days of carbonation). The results show that at pH 2.0 “q” was the lowest for both adsorbents. For the non-carbonated sample (0 days), while the pH increases from 2.0 to 3.2 the “q” increased 30% and kept almost constant until pH 7.4 ( $29.5 \text{ mg.g}^{-1}$ ) (see **Fig. 8**). However,

359

360

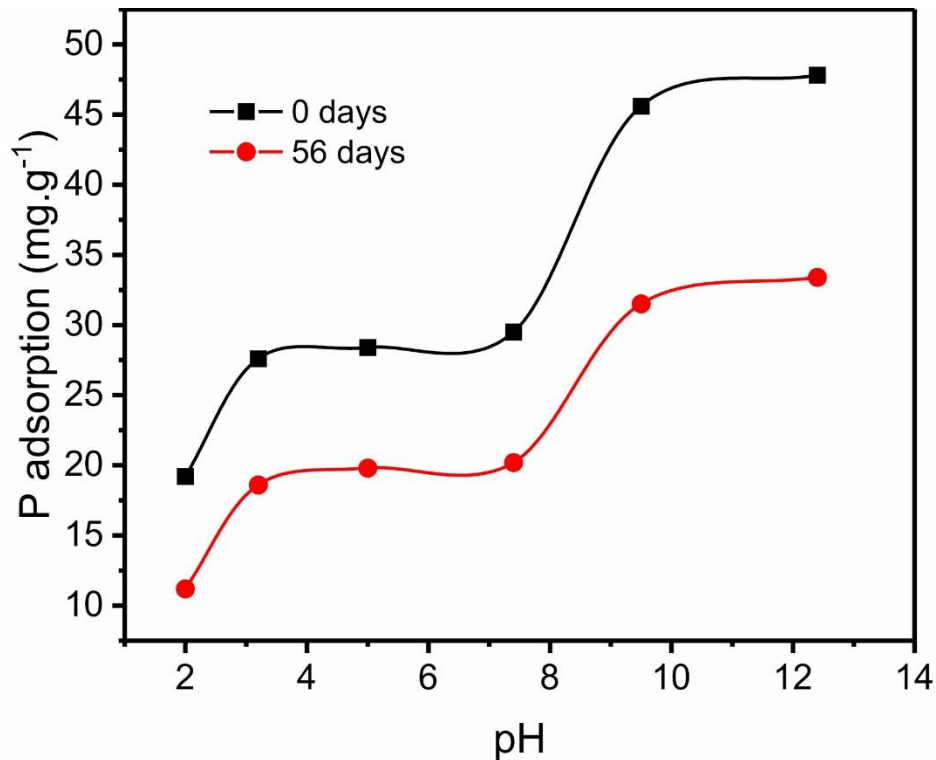
361

362

363



364 when the pH increases from 7.4 to 9.5, the “ $q$ ” increased by 35% ( $45.6 \text{ mg.g}^{-1}$ ). At pH  
 365 12.4, the adsorption capacity increases slightly and reaches  $47.8 \text{ mg.g}^{-1}$ . The same trend  
 366 was observed for the carbonated sample at 56 days; however, with less efficiency (see  
 367 **Fig. 8**).



368

369 **Fig. 8** - Effect of the pH on P removal using non-carbonated (0 days) and  
 370 carbonated samples (56 days).

371

372 The reason for which each pH has different “ $q_e$ ” value can be explained due to P  
 373 adsorption could be influenced by the presence of  $\text{Ca}^{2+}$  dissolved ions (that is one of the  
 374 majority element in concrete waste). Calcium(II) ions can react with the phosphate  
 375 species present in the solution to form the solid calcium phosphate (Yuan et al., 2015).  
 376 As was aforementioned, the presence of the phosphate species mainly depends on the  
 377 solution pH values (Yuan et al., 2015). When pH value is about 9.5,  $\text{HPO}_4^{2-}$  is the  
 378 dominant specie in the solution (Yuan et al., 2015). Yan *et al.* (2007) pointed out that at  
 379 higher pH values, calcium phosphate precipitation is the primary mechanism for P  
 380 removal from aqueous solution.

381 The literature describes that the concentration of dissolved  $\text{Ca}^{2+}$  decreases when  
382 the pH initial value increases and this provokes the inhibition of calcium phosphate  
383 precipitation and then reduces phosphate adsorption (Yan *et al.* 2007; Yuan *et al.*, 2015).  
384 This behavior was observed in this work for both non-carbonated and carbonated  
385 samples (see **Table. 2**).

386

387 **Insert Table 2**

388

389 Based on these results, it can be pointed out that, at higher pH values, calcium  
390 phosphate precipitation is one of the most predominant mechanisms in P removal from  
391 aqueous solution by using concrete-waste adsorbent. It is reported that P adsorption is  
392 hindered in alkaline environment because of the competition for surface active sites by  
393 hydroxide and phosphate ions (Johansson and Gustafsson, 2000). The acid pH helps  
394 the concrete body to release  $\text{Ca}^{2+}$  ions into the solution which react with the P causing  
395 the precipitation of  $\text{Ca}_3(\text{PO}_4)_2$  (Yan *et al.* 2007). The enhance in P removal above pH 7.8  
396 could be due to the formation of OH enriched complexes precipitating calcium phosphate  
397 (Yan *et al.* 2007).

398

### 399 **3.2.3 Effect of the temperature on P removal**

400

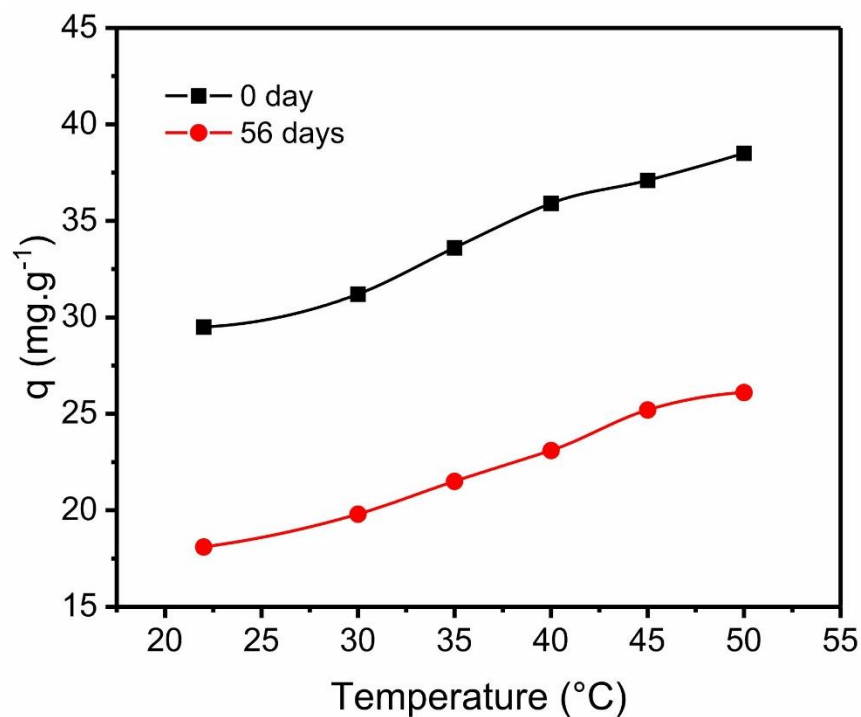
401 P removal onto concrete-waste adsorbents was also studied as a function of  
402 temperature. Results obtained in this study are given in **Fig. 9**. As shown in **Fig. 9**, the  
403 adsorption capacity increased as the temperature increased, and that the adsorption of  
404 P by the concrete-waste adsorbents most likely occurs through chemical interactions  
405 rather than physical interactions.

406 **Fig. 9** shows that at 22°C, the P adsorption was 18.1 and 29.5 mg g<sup>-1</sup> for  
407 carbonated and non-carbonated samples, respectively. When the temperature increase  
408 from 22° to 50°C the adsorption capacities increased to 26.1 and 38.4 mg g<sup>-1</sup> for

409 carbonated and non-carbonated samples, respectively, corresponding to an increase in  
 410 the order of 44% and 30% for both carbonated and non-carbonated samples,  
 411 respectively. These results agree with early report (Li et al., 2016).

412 Although the temperature is an essential parameter in the P adsorption over  
 413 concrete samples, the increase in the temperature results in a very high operational cost  
 414 for the adsorption process, therefore, 22°C was selected as an optimum temperature for  
 415 the kinetic and equilibrium experiments.

416



417

418 **Fig. 9** - Effect of the temperature on P removal using non-carbonated (0 days)  
 419 and carbonated samples (56 days).

420

### 421 **3.2.4 Kinetic study of the adsorption**

422

423 Kinetic adsorption process gives insights about the interaction between the used  
 424 adsorbent and adsorbate and its importance in the process to obtain the equilibrium.

425 P ions adsorption on both concrete-waste adsorbents were very fast at the  
 426 beginning of the process and reached 50% of P removal in 2.19 and 5.79 min for 0-day

427 and 56-day adsorbents, respectively; afterward, the P was slowly adsorbed achieving  
428 95% of removal in 71.54 and 103.7 min for non-carbonated (0-day) and carbonated (56-  
429 days) adsorbents, respectively.

430 Adsorption of P on both samples can be split into three stages:

431 (i) the rapid adsorption at the beginning of the kinetic, due to many available  
432 active sites that easily adsorb P ion species on the surface of the concrete  
433 adsorbents;

434 (ii) the slow adsorption in the second stage which suggests that the active sites  
435 are becoming saturated;

436 (iii) The equilibrium characterized by a plateau, which corresponds to the  
437 saturation of the adsorbent sites.

438

439 It is worth to note that in the calcium-rich adsorbents such as concrete, phosphate  
440 is also precipitated and can be removed by an ion-exchange mechanism between  
441 calcium species present at the surface of the adsorbents and phosphate species in  
442 solution, rather than a fixation at the surface of the adsorbents as commonly found in the  
443 literature (Rahnemaie and Hiemstra, 2006; Sabah and Majdan, 2009; Kudayarova,  
444 2010). Therefore, the adsorption mechanism in this study is different from that of  
445 conventional adsorbents listed in the literature, such as activated carbons. The dissolved  
446  $\text{Ca}^{2+}$  from the dissolution of  $\text{CaCO}_3$ ,  $\text{CaO}$  and  $\text{Ca}(\text{OH})_2$  are preferably precipitated by P  
447 species (in phosphate form) in high pH solution, which gives a high initial rate of sorption.

448 Therefore, the adsorption of P onto concrete-waste adsorbents probably resulting  
449 from a significant presence of many functional groups and oxides that are effectively  
450 involved in the P capture as well as ion exchange mechanisms (Choi et al., 2016).

451 The fitting curves were analyzed by three models, pseudo-first-order, pseudo-  
452 second-order, and general order kinetic model. The fitting curves and their parameters  
453 are exhibited in **Fig. 10** and **Table 3**. It appears that the kinetic data is more suitable to  
454 characterize the General order model.

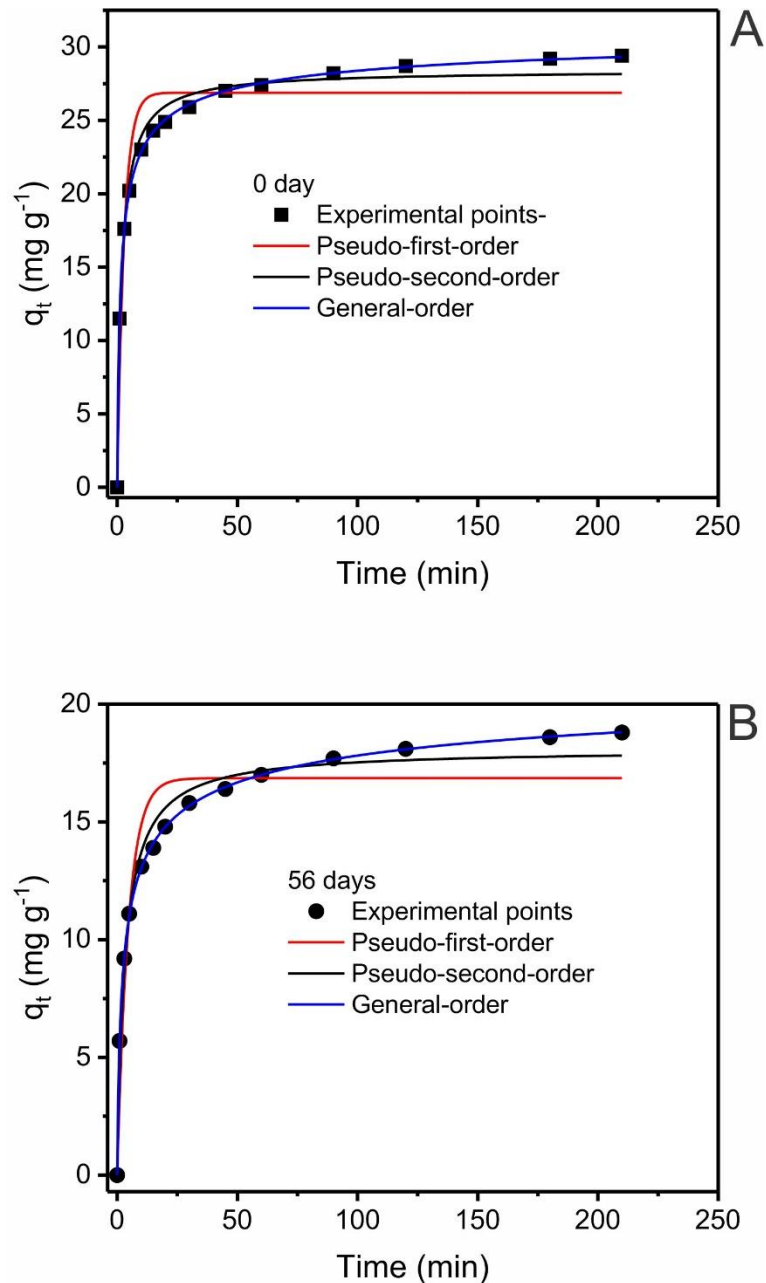


**Fig. 10** - Kinetic curves for adsorption of P (A) non-carbonated and (B) carbonated samples.

### Insert Table 3

The fitness of the kinetic models was evaluated according to the adjusted determination coefficient ( $R^2_{\text{adj}}$ ), and standard deviation of residues (SD). Lower SD and higher  $R^2_{\text{adj}}$  values imply a smaller difference between experimental and theoretical  $q$

464 values (which is given by the models) and therefore have the best suitable model.  
465 According to **Fig. 10** and **Table 3**, the general order kinetic model was the most suitable  
466 (for both adsorbents) model which best represent the experimental kinetic data, since  
467 they presented lower SD (0.1203 and 0.09344) and higher  $R^2_{adj}$  values (0.9998 and  
468 0.9997), for both 0-day and 56-day adsorbents, respectively (see **Table 3**). This indicates  
469 that the  $q_t$  predicted by the General order model presented the closest calculated values  
470 compared to the experimental  $q_t$ .

471 The general order kinetics describes that the order of adsorption should be the  
472 same as that of a chemical reaction which makes more sense in P removal onto  
473 concrete-waste adsorbents. It is well-known that P species (phosphate anions) are  
474 chemisorbed on the surface of metal-containing soil sorbents with the formation of hardly  
475 soluble metal–phosphate complexes (Rahnemaie et al., 2006; Kudeyarova, 2010).

476

### 477 **3.2.5 Equilibrium models**

478

479 The determination of the adsorption isotherm presents an indispensable role in  
480 the design of both methods fixed bed and batch adsorptions, besides allows to a better  
481 understanding of the whole adsorption process.

482 There are several isotherm models to evaluate equilibrium studies. In this  
483 research, Langmuir, Freundlich, and Liu isotherms were chosen to evaluate the fitness  
484 of the P adsorption over two concrete-waste adsorbents, a non-carbonated sample and  
485 carbonated one. The aim is to evaluate how the carbonation process affected P  
486 maximum adsorption capacity.

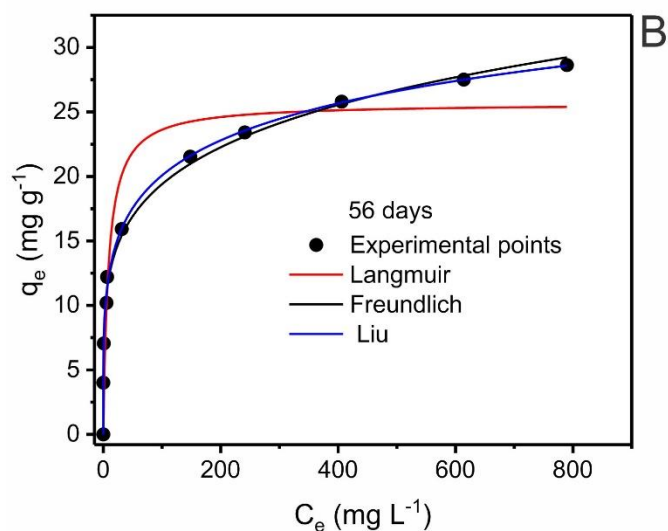
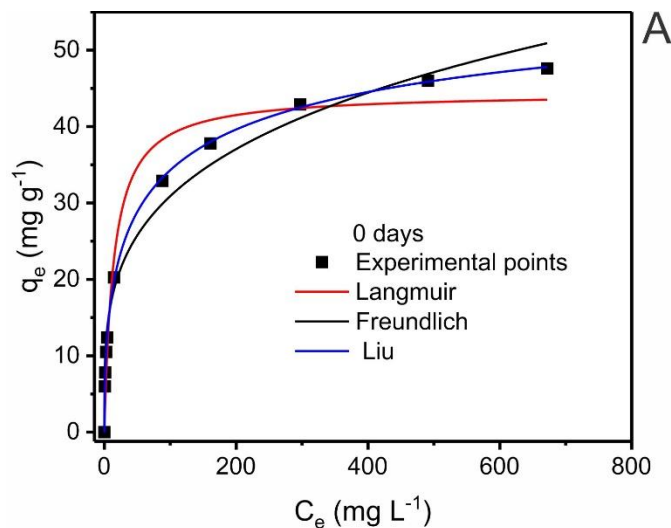
487 The P adsorption isotherm curves and their parameters for the adsorbents at 0  
488 and 56 days of carbonation are displayed in **Fig. 11** and **Table 4**. The fitness of the  
489 models was evaluated using the  $R^2_{Adj}$  and SD similar to the kinetic studies discussed  
490 above.

491 In the light of  $R^2_{Adj}$  and  $SD$  values, the equilibrium adsorption is more suitable to  
 492 be described with Liu model, because it has the highest  $R^2_{adj}$  and the lowest  $SD$  values,  
 493 in comparison with Langmuir and Freundlich models. This finding means that Langmuir  
 494 and Liu's isotherms show lower goodness of fit, which means that these models do not  
 495 describe well the adsorption process of P for concrete adsorbent used in this work under  
 496 applied conditions. Likewise, the  $q$  values provided by the Liu model were closer to those  
 497 obtained experimentally.

498

499

500



501

502 **Fig. 11** – Adsorption isotherm curves of P for (A) 0 day and (B) 56 days.

503

504 **Insert Table 4**

505

### 506 **3.2.5 Adsorbent efficiency**

507

508 The evaluation of the effectiveness of the adsorption process depends on the  
509 adsorbent efficiency in terms of how it can uptake the desired pollutant. The adsorbent  
510 efficiency is usually performed from the comparison of the values of maximum adsorption  
511 capacities. To make a comparison among the results found in this paper, supplementary  
512 **Table 1** summarizes the adsorption capacities and the main conditions and conclusions  
513 of some concrete/cementitious adsorbent materials in P removal from aqueous media in  
514 the literature.

515 The non-carbonated and carbonated samples (0 and 56 days, respectively)  
516 exhibited  $Q_{\max}$  values of 63.85 and 63.83 mg g<sup>-1</sup> (obtained from Liu isotherm model)  
517 which are among the highest adsorption capacities of that of other low-cost adsorbents  
518 cited in the literature (see supplementary **Table 1**).

519 The reasons for different  $Q_{\max}$  values for P adsorption might be justified by the  
520 fact that these works have used different experimental conditions such as different  
521 adsorbents, contact time, pH, and different isotherm models used (Langmuir, Liu, etc.).  
522 supplementary **Table 1** also highlights from different experimental conditions ones can be  
523 obtained different findings and conclusions.

524 However, it is possible to infer that, based on supplementary **Table 1**, the  
525 adsorbents used in this paper presented pretty good effectiveness for P adsorption and  
526 recovery from aqueous effluents since it is abundant and cheap to be enabled for  
527 adsorption experiments.

528

### 529 **3.2.6 Possible mechanisms of phosphate removal**



530

531 The adsorption of P species ions on the negatively-charged surface of concretes  
532 and the precipitation of phosphate compounds can both respond for the majority of P  
533 removal and recovery. Additionally, electrostatic interactions might also take place in the  
534 mechanism of P adsorption on concrete. The importance of each adsorption mechanism  
535 is probably determined by the pH of the adsorbate solution (Choi et al., 2016; Tracz et  
536 al., 2019).

537 Before adsorption tests, the initial pH values of P solutions were around 7.6.  
538 However, after adsorption tests, the pH was always higher than 10.0; this indicates that  
539 the surfaces of both adsorbents were negatively charged.

540 Under very acid solution, the concrete surface is positively charged, which favors  
541 the uptake of negatively charged phosphate ions due to the adsorption reactions and the  
542 electrostatic attraction.

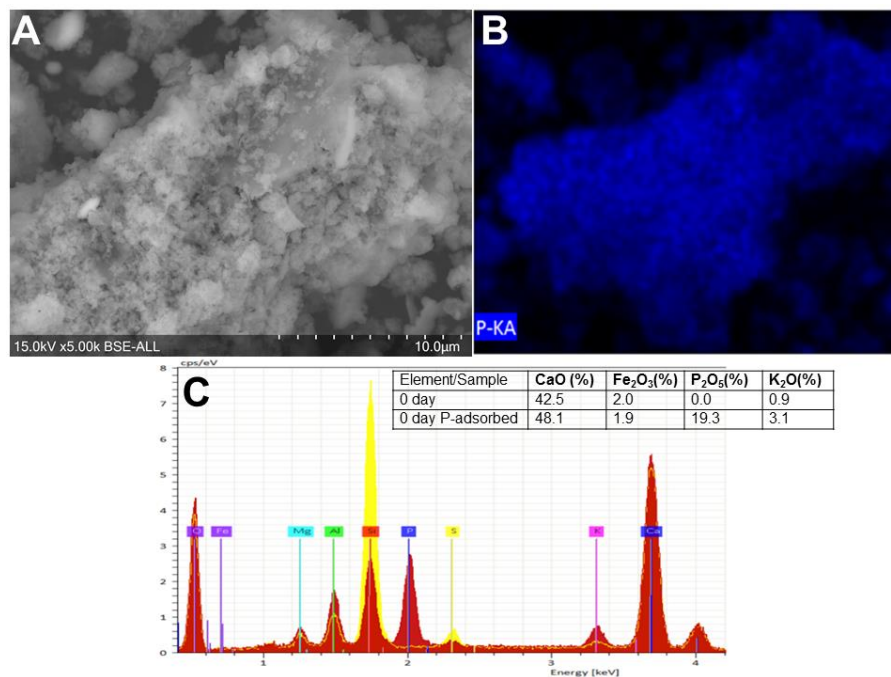
543 In the surface complexation mechanism, the adsorption of phosphate takes  
544 place, on concrete surface, when part of hydroxyl groups on its surface from different  
545 oxides (e.g., Fe—O—H, Ca—O—H..., etc) could be replaced by P anions and  
546 subsequently the new Fe—O—P and Ca—O—P inner-sphere complexes could be formed  
547 (Rahnemaie et al., 2006). Inner sphere complexes indicate that they are strongly bonded  
548 to highly structure mineral surfaces and P via covalent binding (Rahnemaie et al., 2006;  
549 Sabah and Majdan, 2009). The  $\text{H}_2\text{PO}_4^-$  and  $\text{HPO}_4^{2-}$  can also react with some oxides (eg.,  
550 Si—O—H, Ca—O—H, Al—O—H...etc) via hydrogen bonding according to follows (Sabah  
551 and Majdan, 2009).

552 Deng and Wheatley (2018) reported the same findings concerning the P  
553 adsorption mechanism on concrete-waste adsorbents. They showed that the P species  
554 were mostly adsorbed due to the presence of the oxides of Ca, Al, Mg, and Fe, which  
555 can effectively bind with P (e.g., phosphate) in aqueous solution.

556 Another mechanism of P removal in concrete - P solution system is the calcium  
557 and metal oxides precipitation, being  $\text{Ca}^{2+}$  the major element that influence in the P

558 precipitation in the form of calcium-phosphate. Concrete-waste adsorbent leaches out  
 559  $\text{Ca}^{2+}$ , and  $\text{Ca}^{2+}$  reacts with  $\text{HPO}_4^{2-}$  and  $\text{PO}_4^{3-}$  to form calcium phosphate. The same  
 560 precipitation mechanism might happen for other metals oxides such as Fe, Al, Mg, etc.

561 The **Fig. 12** shows the SEM and EDS mapping of the main elements found in  
 562 non-carbonated concrete loaded with phosphate. It shows that the main element is CaO  
 563 and the presence of P was detected in sample used in the P adsorption, highlighting that  
 564 non-carbonated sample successfully adsorbed the P.



565

566 **Fig. 12** SEM and EDS mapping of the non-carbonated slurry concrete loaded P.

567

### 568 **3.2.7 Environmental analysis (Leaching out tests) of concrete samples**

569

570 The leaching out method was used to investigate the leaching of trace elements  
 571 from the non-carbonated (0 days) and carbonated (56 days) concrete-waste adsorbent  
 572 used in this work and the target trace elements are presented in **Table 5**. The leached  
 573 out elements, even in tiny contents, can decrease the P removal efficiency due the  
 574 competition for adsorption. Moreover, the effect of coexisting elements (with different  
 575 concentrations) on P removal efficiency is a complex process, and it is difficult to

576 generalize on removal performance based only on laboratory scale experiments.  
577 Furthermore, the leaching of elements contained in the concrete adsorbents needs to be  
578 further investigated for the case of real polluted waters.

579 It can be seen that, despite the variability, all-metal levels released in the water  
580 from both concrete samples were within the allowable limits for agricultural soil irrigation  
581 purposes preconized by FAO (Ayers and Westcot 1985). Among all metals evaluated in  
582 **Table 5**, only the molybdenum exceeds the limit imposed by FAO (Ayers and Westcot  
583 1985) in terms of waters used for irrigation. The rest of metals are below the limit which  
584 recommends maximum concentrations of trace elements in irrigation water. However,  
585 Ca and K seem to exceed the limits preconized by FAO (Ayers and Westcot 1985).

586 However, it does not represent a hazard because in this case, we are handling  
587 with wastewaters. Besides, for the leaching out tests were used a considerable amount  
588 of concrete (dosage of  $30.0 \text{ g.L}^{-1}$ ) compared with those amounts used for the kinetic and  
589 equilibrium tests (dosage of  $5.00 \text{ g.L}^{-1}$ ); therefore it is expected that the real valor would  
590 be lower than those presented in **Table 5**. In general, non-carbonated samples leached  
591 out higher element contents when compared to carbonated sample (see Table 5). The  
592 carbonation process improves the mechanical properties of the concrete-waste, which  
593 difficult the leaching elements out of the concrete matrix.

594

### 595 ***3.2.8 Viability and advantages of use P adsorbed on concrete as potential P-*** 596 ***fertilizer***

597 Cementitious waste come as promising materials for the designing of inexpensive  
598 phosphate adsorbents because they contain many oxides and alkali calcium compounds  
599 that are effective in phosphate capture and recovery.

600 The conventional processes employed today for P removal are chemical  
601 precipitation, ion exchange resins, biological activated sludge. These processes can  
602 achieve high efficient results for P removal; however, they present high costs and difficult

603 to be implemented. Adsorption process is easy to be implemented and is economically  
604 viable.

605 Concrete-waste adsorbents have shown to have high P-removal performance  
606 and therefore can be used as an inexpensive P recovery agent. Moreover, its natural  
607 and environmentally friendly features make it suitable to be used as a fertilizer or soil  
608 conditioner such to correct soil acidity. Concrete contains many essential macronutrients  
609 (P, K, Ca, Mg), micronutrients (Fe, Mn and B) and some beneficial elements (Si, Na) for  
610 plant growth and therefore it is useful for agricultural purposes.

611 Besides, the use of P-loaded adsorbent as a fertilizer could be more cost-effective  
612 than regenerating it; since the regeneration process can reach up to 70% of the total  
613 operating and maintenance cost of an adsorption system (Goh et al., 2008). However,  
614 future works should be done concerning the study of concrete adsorbent regeneration.

615

### 616 **3.2.8 Adsorbent and adsorption process cost assessment**

617

618 Economic study is an important factor to be taken into account for determining  
619 the applicability of an adsorbent in a wastewater treatment process. The economic  
620 viability of the adsorption process depends mainly on the cost of the used adsorbent.

621 However, since the concrete adsorbent is a waste, it means that there is no cost  
622 associated with its preparation and with equipment for instance. Therefore, it is  
623 highlighted that there will be a cost associated with the transportation of the waste to the  
624 wastewater treatment plant. When it is compared to other low-cost adsorbents reported  
625 in the literature, the adsorption process by using concrete waste adsorbents can be  
626 economically viable since it is an abundant waste and it is not necessary to spend energy  
627 and chemicals to process it. Moreover, when compared with the most popular adsorbent  
628 (commercial activated carbons), it can reach 111\$/kg, which is too high. However, low  
629 cost activated carbons can be prepared at the cost of 14.36\$/kg (Reza et al., 2014).

630 Bhatnagar et al., (2013) prepared a low-cost adsorbent by using a bio-waste treated with  
631  $H_3PO_4$  and calculated its preparation costs at 0.5 \$/kg.

632 Therefore, to achieve a circular economy, this research shows that it is possible  
633 to use a low-cost and eco-friendly adsorbent for recovering P from aqueous effluents. To  
634 close the cycle, the P-loaded concrete can be potentially used as fertilizer which makes  
635 the process more economically sustainable.

636

#### 637 **4. Conclusion**

638

639 In this work, the effect of the carbonation process on physicochemical properties  
640 and in the adsorption of phosphate on the concrete slurry powder was investigated.

641 General order kinetic provided the better fitting model for the adsorption behavior  
642 of P onto both non-carbonated and carbonated concrete samples. The equilibrium  
643 adsorption data were better fitted by Freundlich isotherm model describing heterogeneity  
644 in the adsorption of P onto concrete-waste adsorbents.

645 P removal was mainly ruled by chemical adsorption through inner-sphere  
646 complexation and P precipitation on the surface of concrete adsorbent having  $Ca^{2+}$  as an  
647 essential element in the adsorption mechanism. Compared with other phosphate  
648 adsorbents, both non-carbonated and carbonated concrete may be an economical and  
649 efficient adsorbent.

650 The non-carbonated sample gave a high adsorption capacity of P (47.6 mg P per  
651 g of concrete, experimental value) and presenting a fast and high initial adsorption,  
652 reaching 72% of P removal only in 5 min at 22°C, while carbonated sample showed a  
653 value of 30.6 mg g<sup>-1</sup> as adsorption capacity at the same experimental conditions.

654 Non-carbonated and carbonated concrete adsorbents showed to have of the  
655 highest phosphate-removal performance between many adsorbents found in the  
656 literature; therefore, concrete slurries can be used widely as an inexpensive phosphate-  
657 recovery adsorbent.

658            Additionally, the application of non-carbonated and carbonated concrete waste,  
659 loaded with P, as potential fertilizers can be an interesting and environmentally approach  
660 for reusing this kind of waste.

661            The environmental analysis highlighted that the adsorbents did not leach out  
662 heavy metals above the allowable limits preconized by FAO for irrigation waters.  
663 However, aspects related to monitoring the presence and mobility of heavy metals on  
664 soil must be better addressed and monitored.

665

### 666 **Acknowledgment**

667

668 The authors thank the Coordination of Improvement of Higher Education Personnel  
669 (CAPES, Brazil) and Foundation for Research Support of the State of Rio Grande do Sul  
670 (FAPERGS), National Council for Scientific and Technological Development (CNPq,  
671 Brazil) for financial support and sponsorship. Dr Glaydson Simões dos Reis is grateful  
672 to the CAPES for the postdoctoral scholarship granted through the National Postdoctoral  
673 Program (PNPD). We are also grateful to Chemaxon for giving us an academic research  
674 license for the Marvin Sketch software, Version 19.20.0, (<http://www.chemaxon.com>),  
675 2019 used for calculation of phosphate species distribution.

676

677

678

### 679 **References**

680

681 Abass A., Olajire A., 2013. A review of mineral carbonation technology in sequestration  
682 of CO<sub>2</sub>, J. Petroleum Sci. Eng. 109, 364–392.

683 Alavaisha E., Manzoni S., Lindborg R., 2019. Different agricultural practices affect soil  
684 carbon, nitrogen, and phosphorous in Kilombero –Tanzania, J. Environ. Manage.  
685 234, 159–166.

686 Ayers R.S., Westcot D.W., 1985. Water quality for agriculture, Food and Agriculture  
687 Organization of the United Nations, Rome, Italy.

- 688 Aynur K., Ulubeyli S., 2016. Current Methods for the Utilization of the Fresh Concrete  
689 Waste Returned to Batching Plants, *Procedia Eng.* 161, 42– 46.
- 690 Bhatnagar, A., Hogland, W., Marques, M., Sillanpää, M. 2013. An overview of the  
691 modification methods of activated carbon for its water treatment applications,  
692 *Chem. Eng. J.* 219, 499–511
- 693 Bravo M., de Brito J., Evangelista L., Pacheco J., 2018. Durability and shrinkage of  
694 concrete with CDW as recycled aggregates: Benefits from superplasticizer's  
695 incorporation and influence of CDW composition. *Construc. Build. Mater.* 168,  
696 818–830.
- 697 Burianek P., Skalicky M., Grunwald A., 2014. Phosphates adsorption from water by  
698 recycled concrete. *Geo. Sci. Eng.* 60, 1–8.
- 699 Cardoso R., Silva R.V., de Brito J., Dhir R., 2016. Use of recycled aggregates from  
700 construction and demolition waste in geotechnical applications: A literature  
701 review. *Waste Manag.* 49,131–145.
- 702 Choi J., Chung J., Lee W., Kim J-O., 2016. Phosphorous adsorption on synthesized  
703 magnetite in wastewater, *J. Ind. Eng. Chem.* 34, 198–203.
- 704 Deng Y., Wheatley A., 2018. Mechanisms of Phosphorus Removal by Recycled Crushed  
705 Concrete, *Int. J. Environ. Res. Public Health* 15, 357.
- 706 dos Reis G.S., Sampaio C.H., Lima E.C., Wilhelm M., 2016. Preparation of novel  
707 adsorbents based on combinations of polysiloxanes and sewage sludge to  
708 remove pharmaceuticals from aqueous solutions, *Colloids and Surfaces A:  
709 Physicochem. Eng. Aspects* 497, 304–315.
- 710 Egemose S., Sønderup M.J., Beinthin M.V., Reitzel K., Hoffmann C.C., Flindt M.R., 2012.  
711 Crushed concrete as a phosphate-binding material: a potential new management  
712 tool. *J. Environ. Qual.* 3, 647-53.
- 713 Goh K.H., Lim T.T, Dong Z., 2008. Application of layered double hydroxides for removal  
714 of oxyanions: a review. *Water Research* 42, 1343–1368.

- 715 Johansson L., Gustafsson J.P., 2000. Phosphate removal using blast furnace slags and  
716 Opoka-mechanism, *Water Res.* 34, 259–265.
- 717 Kasperiski F. M., Lima E.C., Umpierres C. S., dos Reis G. S., Thue P.S., Lima D.R., Dias  
718 S.L.P., Saucier C., da Costa J.B., 2018. Production of porous activated carbons  
719 from *Caesalpinia ferrea* seed pod wastes: Highly efficient removal of captopril  
720 from aqueous solutions, *J. Cleaner Prod.* 197, 919-929.
- 721 Kudayarova A.Y., 2010. Chemisorption of Phosphate Ions and Destruction of  
722 Organomineral Sorbents in Acid Soils, *Eurasian Soil Science* 43, 635–650.
- 723 Leite A.J.B., Lima E.C., dos Reis G.S., Thue P.S., Saucier C., Rodembusch F.S., Dias  
724 S.L.P., Umpierres C.S., Dotto G.L., 2017. Hybrid adsorbents of tannin and APTES  
725 (3-aminopropyl-triethoxy-silane) and their application for the highly efficient  
726 removal of acid red 1 dye from aqueous solutions, *J. Environ. Chem. Eng.* 5,  
727 4307-4318.
- 728 Li F., Wu W., Li R., Fu X., 2016. Adsorption of phosphate by acid-modified fly ash and  
729 palygorskite in aqueous solution: Experimental and modeling, *Appl. Clay Sci.*  
730 132–133, 343–352.
- 731 Lima E.C., Adebayo M.A., Machado F.M., 2015. Kinetic and Equilibrium Models of  
732 Adsorption, in: Bergmann, C.P., Machado, F.M. (Eds.), *Carbon Nanomaterials as*  
733 *Adsorbents for Environmental and Biological Applications*, Springer International  
734 Publishin, New York, United States pp. 33–69.
- 735 Littler J., Geroni J.N., Sapsford D.J., Coulton R., Griffiths A.J., 2013. Mechanisms of  
736 phosphorus removal by cement-bound ochre pellets. *Chemosphere* 90, 1533–  
737 1538.
- 738 Ma H., Guo Y., Qin Y., Li Y-Y., 2018. Nutrient recovery technologies integrated with  
739 energy recovery by waste biomass anaerobic digestion, *Bioresource Technol.*  
740 269, 520–531.
- 741 Nasar N., Payattati B., 2015. *Int. J. Innovative Res. Sci. Eng. Technol*, 1-8.



- 742 Park J.Y., Byun H.J., Choi W.H., Kang W.H., 2008. Cement paste column for  
743 simultaneous removal of fluoride, phosphate, and nitrate in acidic wastewater.  
744 *Chemosphere* 70,1429–1437.
- 745 Rahnemaie R., Hiemstra T., van Riemsdijk W.H., 2006. Inner- and outer-sphere  
746 complexation of ions at the goethite–solution interface, *J. Colloid Inter. Sci.* 297,  
747 379–388.
- 748 Reza, R.A., Ahmed, M.J.K., Ahmaruzzaman, A.K.S.M. 2014. A Non-Conventional  
749 Adsorbent for the Removal of Clofibrac Acid from Aqueous Phase, *Sep. Sci.*  
750 *Technol.* 49, 10, 1592-1603
- 751 Sabah E., Majdan M., 2009. Removal of phosphorus from vegetable oil by acid-activated  
752 sepiolite. *J. Food Eng.* 91, 423–427.
- 753 Sasaki T, Iizuka A., Watanabe M., Hongo T., Yamasaki A., 2014. Preparation and  
754 performance of arsenate (V) adsorbents derived from concrete wastes. *Waste*  
755 *Manage.* 34, 1829–1835.
- 756 Sun D., Hale L., Kar G., Soolanayakanahally R., Adl S., 2018. Phosphorus recovery and  
757 reuse by pyrolysis: Applications for agriculture and environment, *Chemosphere*  
758 194, 682-691.
- 759 Taylor H.F.W., 1978. *The chemistry of cements (in spanish)*, Ed. URMO, Bilbao, Spain.
- 760 Thue P.S., Adebayo M.A., Lima E.C., Sieliechi J.M., Machado F.M., Dotto G.L., Vaghetti  
761 J.C.P., Dias S.L.P., 2016. Preparation, characterization, and application of  
762 microwave-assisted activated carbons from wood chips for removal of phenol  
763 from aqueous solution, *J. Mol. Liq.* 223, 1067–1080.
- 764 Tracz T., Zdeb T., 2019. Effect of Hydration and Carbonation Progress on the Porosity  
765 and Permeability of Cement Pastes, *Materials* 12, 192.  
766 doi: 10.3390/ma12010192
- 767 Umpierrez C.S., Thue P.S., dos Reis G.S., de Brum I.A.S., Lima E.C., de Alencar W.A.,  
768 Dias S.L.P., Dotto G.L., 2018. Microwave activated carbons from Tucumã

- 769 (Astrocaryum aculeatum) waste for efficient removal of 2- nitrophenol from  
770 aqueous solutions. Environ. Technol. 39, 1173-1187.
- 771 Vásquez A., Cárdenas V., Robayo R.A., de Gutiérrez R.M., 2016. Geopolymer based on  
772 concrete demolition waste. Adv. Powder Technol. 27, 1173–1179.
- 773 Wamba A.G.N, Ndi S.K., Lima E.C., Kayem J.G., Thue P.S., Kayem J.G., Robembusch  
774 F.S., Dos Reis G.S., De Alencar W.S., 2017. Synthesis of grafted natural pozzolan  
775 with 3-aminopropyl-triethoxy-silane: preparation, characterization, and  
776 application for removal of Brilliant Green 1 and Reactive Black 5 from aqueous  
777 solution, Environ. Sci. Pollut. Res. 24–27, 21807–21820.
- 778 Wang X.J., Chen J.D., Kong Y.P., Shi X.M., 2014. Sequestration of phosphorus from  
779 wastewater by cement-based or alternative cementitious materials. Water Res.  
780 62, 88–96.
- 781 World Business Council for sustainable development (WBCSD), 2019. Recycling  
782 concrete. [www.docs.wbcSD.org/2009/07/CSI-RecyclingConcrete-FullReport.pdf/](http://www.docs.wbcSD.org/2009/07/CSI-RecyclingConcrete-FullReport.pdf/)  
783 (Accessed 5 July 2019)
- 784 Yan J., Kirk D.W., Jia C.Q., Liu X., 2007. Sorption of aqueous phosphorus onto  
785 bituminous and lignite coal ashes, J. Hazard. Mat.148, 395–401.
- 786 Yuan X., Xia W., An J., Yin J., Zhou X., Yang W., 2015. Kinetic and Thermodynamic  
787 Studies on the Phosphate Adsorption Removal by Dolomite Mineral, Journal of  
788 Chemistry, 853105, 1-8, DOI: 10.1155/2015/853105
- 789 Zha Z., Ren Y., Wang S., Qian Z., Yang L., Cheng P., Hana Y., Wang M., 2018. Phosphate  
790 adsorption onto thermally dehydrated aluminate cement granules, RSC Adv. 8,  
791 19326–19334.
- 792
- 793